

This article was downloaded by:

On: 24 January 2011

Access details: *Access Details: Free Access*

Publisher *Taylor & Francis*

Informa Ltd Registered in England and Wales Registered Number: 1072954 Registered office: Mortimer House, 37-41 Mortimer Street, London W1T 3JH, UK



Journal of Liquid Chromatography & Related Technologies

Publication details, including instructions for authors and subscription information:

<http://www.informaworld.com/smpp/title~content=t713597273>

The Development of Stationary Phase Supports For Liquid Chromatography. I. Examination of the Pore Structure of Zirconia-Silica Composites Using Size Exclusion Chromatography

R. A. Shalliker^a; G. K. Douglas^a

^a Centre for Instrumental and Developmental Chemistry, Queensland University of Technology, Brisbane, Australia

To cite this Article Shalliker, R. A. and Douglas, G. K.(1998) 'The Development of Stationary Phase Supports For Liquid Chromatography. I. Examination of the Pore Structure of Zirconia-Silica Composites Using Size Exclusion Chromatography', *Journal of Liquid Chromatography & Related Technologies*, 21: 12, 1749 – 1765

To link to this Article: DOI: 10.1080/10826079808005889

URL: <http://dx.doi.org/10.1080/10826079808005889>

PLEASE SCROLL DOWN FOR ARTICLE

Full terms and conditions of use: <http://www.informaworld.com/terms-and-conditions-of-access.pdf>

This article may be used for research, teaching and private study purposes. Any substantial or systematic reproduction, re-distribution, re-selling, loan or sub-licensing, systematic supply or distribution in any form to anyone is expressly forbidden.

The publisher does not give any warranty express or implied or make any representation that the contents will be complete or accurate or up to date. The accuracy of any instructions, formulae and drug doses should be independently verified with primary sources. The publisher shall not be liable for any loss, actions, claims, proceedings, demand or costs or damages whatsoever or howsoever caused arising directly or indirectly in connection with or arising out of the use of this material.

**THE DEVELOPMENT OF STATIONARY PHASE
SUPPORTS FOR LIQUID CHROMATOGRAPHY.
I. EXAMINATION OF THE PORE STRUCTURE
OF ZIRCONIA-SILICA COMPOSITES USING
SIZE EXCLUSION CHROMATOGRAPHY**

R. A. Shalliker, G. K. Douglas

Centre for Instrumental and Developmental Chemistry
Queensland University of Technology
G.P.O. Box 2434
Brisbane 4001, Australia

ABSTRACT

In this first part of a two part series, the pore structure of zirconia-silica composite stationary phase supports was examined using size exclusion chromatography. The study found that the pore structure was more complex than pure zirconia surfaces. With these composite materials, the pore dimensions are primarily dependent on the concentration of the silicon doping, the temperature of calcination, and the presence of salts during calcination. Silicon concentration influences the phase crystallization which, in turn, alters the temperature at which micropores transform to mesopores. Calcination in the presence of sodium chloride increased the surface area and pore volume of the support.

INTRODUCTION

The use of zirconia as a chromatographic stationary phase support needs no introduction and has been extensively reviewed.¹ Recently, interest has developed in the use of zirconia-silica composites as stationary phase supports. These materials were first introduced by Kaneko and coworkers,² in 1994, where they illustrated the variation in selectivities for benzene, dimethyl phthalate, and pyridine. The silica-zirconia mixed oxide support prepared by Kaneko and coworkers had an irregular particle shape and was thermally treated at 110°C. This support contained a significant microporous region. Kaneko and coworkers made no attempt to optimize the pore structure of the support and, as a result, mass transfer into the porous region may have been less than ideal.

In previous communications, we described the preparation of spherical zirconia-silica composites³ that were essentially zirconia microspheres coated with silica. However, during calcination it was found that the bulk particles became homogeneous as evidenced by the presence of zircon ($ZrSiO_4$). The concentration of silicon had a direct effect on the crystallization of the zirconia from the amorphous phase to the tetragonal phase ($Zr_{\sigma}-Zr_t$),^{3,4} both the amorphous and the tetragonal phases being stabilised by the addition of various concentrations of silicon. As a result, the pore structure of a silicon doped zirconia composite is distinctly different from that of zirconia after identical thermal treatment.⁵ As the pore structure of inorganic oxides is influenced by the crystal phase, the silicon concentration may dramatically affect the porous structure of the composite material. These materials may, therefore, offer novel properties for liquid chromatography that are dependent upon the thermal history of the support.

In the present study, size exclusion chromatography (SEC) was used to evaluate the pore structure, illustrating the changes as a result of silicon concentration and thermal treatment. Previous studies by Halász and Martin⁶ have shown that size exclusion chromatography offers a reliable method for determining the pore size, surface area, and pore volume of chromatographic stationary phases.

The advantage of such a method is that the true chromatographic surface available for solute molecules can be measured directly, whereas other methods, such as nitrogen sorption or mercury porosimetry, yield results which assume that the same access is granted for a solute molecule as in a chromatographic separation. This may not necessarily be true, particularly for large analytes.

In the following paper, we further extend the examination of the porous structure using nitrogen sorption experiments. From these two studies, we show that the pore structure is dependent on the method of examination and attempt to explain such variance.

EXPERIMENTAL

The surfactants Span 80, Brij 35, and Tween 85 were supplied by the Sigma Chemical Company, Inc. (St. Louis, MO, USA). Sodium metasilicate pentahydrate was obtained from BDH Chemicals Ltd (Poole, England). Zirconyl chloride (99%), urea, and hexamethylenetetramine were supplied by the Aldrich Chemical Company, Inc. (Milwaukee WI, USA). Polystyrene standards with molecular weights 1.8×10^6 , 8.60×10^5 , 4.50×10^5 , 1.85×10^5 , 8.7×10^4 , 4.4×10^4 , 2.8×10^4 , 1.02×10^4 , 3.55×10^3 , and 1.35×10^3 were obtained from Shodex. HPLC grade methanol was obtained from BDH Chemicals (Poole, England) and AR grade dichloromethane was supplied by Ajax Chemicals (N.S.W., Australia). All chromatographic solvents were filtered through a Millipore 0.45 μm filter prior to use.

The preparation of zirconia and the zirconia-silica composites has been described previously.³ In the present work, composite materials were subjected to various calcination processes in an attempt to optimize and study the pore structure. Samples were calcined either as pure composites or as homogeneous mixtures of the composite and sodium chloride according to previously described methods.^{3,4} The calcination procedure involved heating the samples to a temperature of $X-30^\circ\text{C}$ at $350^\circ\text{C}/\text{hour}$ after which the sample was heated to the final temperature X at a rate of $60^\circ\text{C}/\text{hour}$. The materials were then calcined for one hour at temperature X unless indicated otherwise. The calcined composite materials were removed from the furnace immediately following the thermal treatment and allowed to cool rapidly to room temperature. They were then washed in copious quantities of water to remove the sodium chloride, followed by washing in methanol and drying at 110°C .

Particle compositions were determined using Xray elemental analysis coupled to a scanning electron microscope as previously described.⁴ Differential thermal analysis (DTA) was used to determine the temperature of transformation from the amorphous state to a crystalline phase.⁷

The zirconia and zirconia-silica composites were subjected to thermogravimetric analysis (TGA) and DTA using a Setaram TGA 92 at heating rates of 2°C min^{-1} (Setaram, Saint-Cloud, France).

Table 1

**Properties of Each Composite, Si Concentration,
and Phase Transition Temperature**

Composite	Si Concentration (mol%)	Phase Transition Temperature (°C)
ZS10	10.2	837
ZS5	5.0	701

Raman spectra were obtained using a Perkin Elmer System 2000 FT-Raman spectrometer. The FT-Raman spectrometer was equipped with a quartz beamsplitter and a continuous-wave Spectron Laser Systems SL301 Nd:YAG laser emitting at 1064 nm and an InGaAs detector operated at ambient temperature. The mirror velocity was 0.2 cm s^{-1} , and strong Beer-Norton apodisation was used. A notch type Rayleigh filter was installed to provide an extended scan range from $3600\text{-}100 \text{ cm}^{-1}$. Typically, 200 scans were recorded at a resolution of 4 cm^{-1} and laser power of 200 mW.

Chromatographic columns were prepared in $5.0 \text{ cm} \times 0.39 \text{ cm}$ stainless steel column blanks fitted with $2 \mu\text{m}$ stainless steel end frits. A Haskel air driven fluid pump (Haskel Engineering and Supply Co., Burbank, CA, USA.) was used as a packing pump and columns were packed in a downward slurry using a methanol packing solvent, a methanol slurry solvent, and a dichloromethane displacement solvent. Columns were packed until the flow rate became constant.

Chromatographic analysis was performed using a Varian 5000 chromatographic system fitted with a $10 \mu\text{m}$ Valco injection port and a fixed wavelength UV detector set at 254 nm. Size exclusion experiments were performed by injecting polystyrene standards of various molecular weights (0.5 mg mL^{-1}) into a dichloromethane mobile phase.

Flow rates were approximately 0.2 mL min^{-1} . The exact flow rate during the elution of each polystyrene standard was recorded during elution and elution volumes were corrected for actual flow rates. All chromatographic experiments were carried out at $23^\circ\text{C} \pm 1^\circ\text{C}$ and were replicated. Mobile phases were sparged with helium.

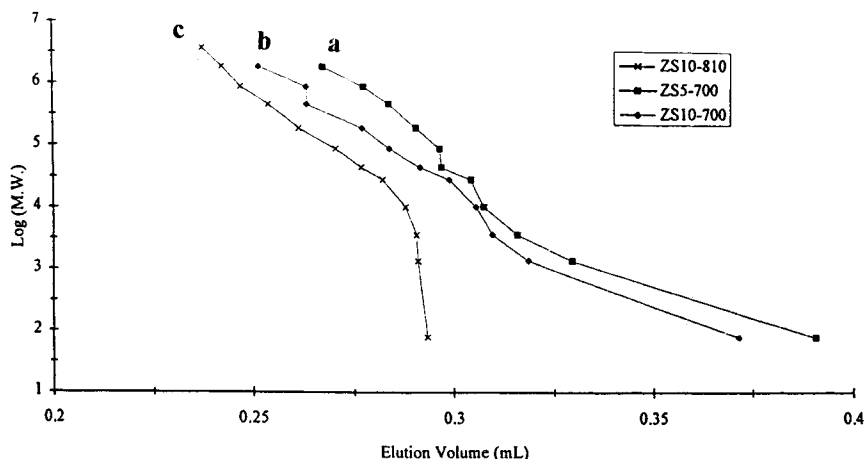


Figure 1. Size exclusion curves on composite ZS5-700 (a), ZS10-700 (b), and ZS10-810 (c). Mobile phase, 100% dichloromethane, solutes polystyrene (0.5 mg/mL), detection 254 nm.

For ease of discussion, the stationary phases examined chromatographically will be referred to using abbreviations such as ZS10-700, which refers to a composite material with 10% Si concentration calcined at 700°C without salt, and ZS10-700NaCl refers to the same material calcined in the presence of sodium chloride.

RESULTS AND DISCUSSION

DTA^{3,4,7-11} and Raman spectroscopy^{3,4,12} are useful for determining phase transitions of composite materials during thermal treatment. Differential thermal analysis showed that the phase transition temperature, as indicated by the exothermic glow peak, occurred at 701°C and 837°C for each composite (Table 1). Raman spectroscopy verified that a zirconia phase change from the amorphous state to the tetragonal state (Zr_{t-t}) occurred at this glow transition temperature.⁴ The exact location of the exothermic 'glow' peak has been shown to be influenced by the concentration of silicon in the matrix.⁴

Calcination of inorganic oxides in the presence of sodium chloride^{5,13} (or salts in general) have been shown to be useful for controlling the pore structure of zirconias. In the present study, identification of the crystalline phase using

Table 2

The Effect of Calcination Temperature on the Pore Structure of Zirconia-Silica Composites Calcined Without Sodium Chloride

Stationary Phase	Calcination Temperature (°C)	p_m (nm)	$\log(\sigma)$	S_a (m^2g^{-1})	V_p (mLg^{-1})	Crystal Phase
ZS5-700	700	4.7	1.23	57.4	0.0678	Zr_t
ZS10-700	700	8.9	1.13	51.1	0.1138	Zr_a
ZS10-810	810	56.2	0.48	2.75	0.0386	Zr_t

Raman spectroscopy showed that the presence of sodium chloride during the calcination process decreased the phase crystallization temperature. Such a result is particularly important for studies involving pore structure as the pore size is largely determined by calcination during which crystallization and particle sintering occur. The crystalline phase of each composite is given in the results corresponding to the pore structure studies where appropriate.

The chromatographically available pore structure of each zirconia-silica composite stationary phase was evaluated using the size exclusion elution behaviour of narrow molecular weight distribution polystyrene standards in a dichloromethane mobile phase. The pore structure was evaluated after calcination with and without sodium chloride as previously studied for pure zirconia.¹³ Where appropriate, composite materials have been compared to pure zirconia. The size exclusion curves for the zirconia-silica composites calcined at 700°C in the absence of sodium chloride are shown in Figure 1. Pore size distributions were calculated from the size exclusion data for each of the stationary phases. The mean pore diameter (P_m) and the standard deviation ($\log \sigma$) for each of the stationary phases was calculated by plotting the sum of residues versus the log of the pore diameter on probability paper.⁶ The probability plots (not shown) for each of the zirconia-silica samples resulted in a scatter of points along a straight line with some variation at the extremes, indicating the pore size distribution was approximately normal. The mean pore diameters determined from the probability plots are presented in Table 2, together with the standard deviations. Specific surface areas (S_a) were determined using the mean pore diameter according to the method of Halász and Martin⁶ and these results are also given in Table 2 as are the specific pore volumes (V_p) and crystalline phase.

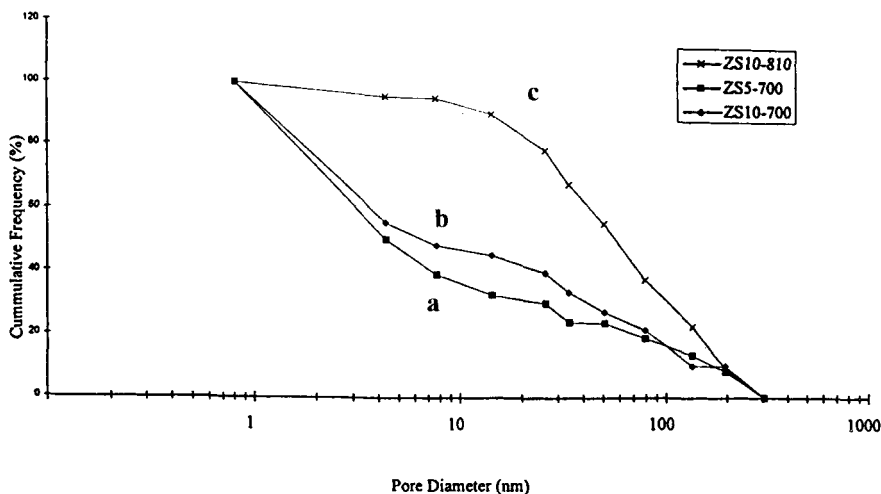


Figure 2. Cumulative pore frequency plots derived from the size exclusion data presented in Figure 1. Composite ZS5-700 (a), ZS10-700 (b), and ZS10-810 (c).

The small inclusion volume on the size exclusion curves of both composites calcined at 700°C is an indication that there is a significant number of micropores or small mesopores. This is further illustrated more graphically by examining the cumulative frequency plots in Figure 2, which show that 50% of the pores are less than 4 nm in diameter. A microporous contribution would be expected for these surfaces as calcination of the ZS10-700 composite did not cause crystallization to the tetragonal form and ZS5-700 composite was calcined at the same temperature as the crystallization temperature. Therefore, only a small degree of pore sintering would be expected. The absence of a distinct exclusion region indicates that there is a macroporous contribution and this is shown in greater detail by examining the cumulative frequency plots in Figure 2. Surprisingly, 20% of the pores were in excess of 80 nm in diameter. By contrast, microporous zirconia exhibited no macroporous structure.^{5,14}

As a result of the microporous contribution, these zirconia-silica composites had high specific surface areas (Table 2). For comparison, a zirconia sample previously examined¹³ using the same calcination conditions had a pore diameter of 20 nm with a surface area of 10.2 m²·g⁻¹ and specific pore volume 0.0511 mL·g⁻¹. Pure zirconia, however, has a phase transition temperature at approximately 450°C and, hence, calcination at 700°C results in particle crystallization, which leads to the loss of micropores¹⁴ and a subsequent reduction in surface area.

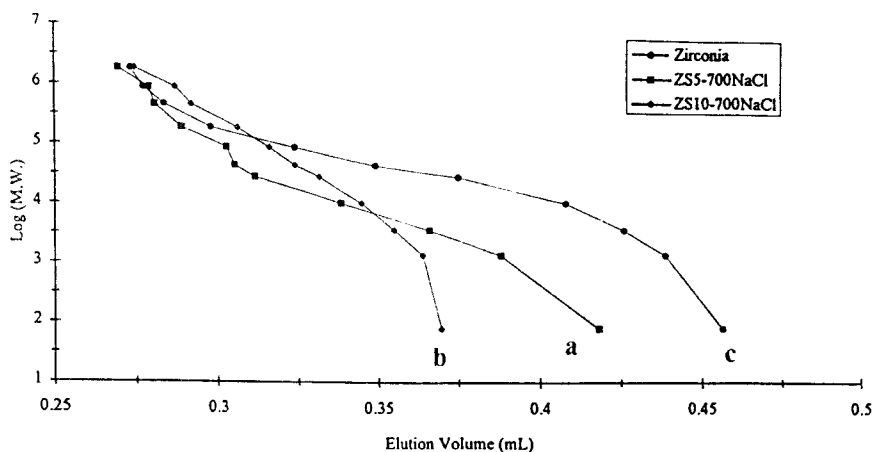


Figure 3. Size exclusion of polystyrenes illustrating the effect of silica concentration on the size exclusion curve for composites calcined at 700°C in a 1:1 mix of composite:NaCl (w/w). ZS5-700NaCl (a), ZS10-700NaCl (b), ZrO₂ (c). Conditions as in Figure 1.

Increasing the calcination temperature altered the surface structure of the zirconia-silica composite significantly. Thus, composite ZS10 calcined at 810°C for one hour showed a dramatic change in the polystyrene size exclusion behaviour (Figure 1). The inclusion limit increased substantially, such that all molecular weights less than 1.0×10^4 daltons eluted within the inclusion volume. The pore volume decreased quite significantly as the results in Table 2 indicate.

The cumulative frequency plot in Figure 2 shows that the microporosity was essentially eliminated and the resulting mean pore diameter increased from 8.9 nm to 56.2 nm. The surface area decreased from $51.1 \text{ m}^2\text{g}^{-1}$ to $2.7 \text{ m}^2\text{g}^{-1}$ with a subsequent decrease in specific pore volume from 0.1138 mLg^{-1} to 0.0386 mLg^{-1} . This result shows that the stability of the surface is greatly affected by thermal treatment.

The size exclusion behaviour on these surfaces and the subsequent pore dimensions indicate that efficient chromatography would be difficult. The rapid change in surface properties with thermal treatment may lead to surfaces which have poor surface reproducibility. In addition, the microporous contribution of the amorphous materials may lead to slow solute diffusion into and out of the pores.

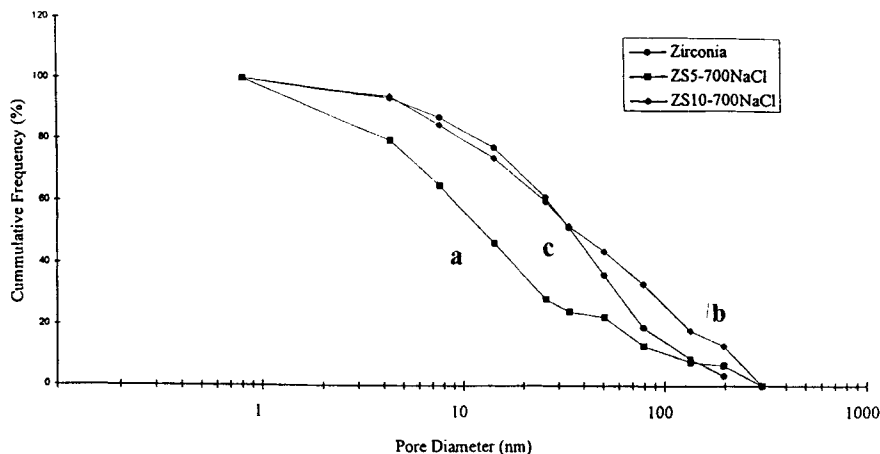


Figure 4. Cumulative pore frequency plots derived from the size exclusion data presented in Figure 3. Stationary phase ZS5-700NaCl (a), ZS10-700NaCl (b), ZrO_2 (c).

Table 3

Pore Dimensions of the Zirconia Silica Composites and Pure Zirconia Calcined at 700°C in the Presence of Sodium Chloride (1:1 Support:NaCl)

Stationary Phase	P_m (nm)	$\log(\sigma)$	S_a ($m^2 g^{-1}$)	V_p ($mL g^{-1}$)	Crystal Phase
ZS5-700NaCl	13.3	0.72	35.4	0.1178	Zr_t
ZS10-700NaCl	39.8	0.69	5.9	0.0589	Zr_t
Zr700NaCl	28.1	0.38	19.2	0.1343	Zr_m

The size exclusion curves for the zirconia-silica composites calcined in the presence of sodium chloride are shown in Figure 3. Pore size distributions, surface areas and specific pore volumes were measured according to the procedure described above and this data is presented in Table 3. The probability plots for each of the zirconia-silica samples, which are not shown, resulted in a scatter of points along a straight line with some variation at the extremes, indicating the pore size distribution was approximately normal.

The first significant conclusion that can be drawn from the size exclusion curves depicted in Figure 3 is that the salt impregnated zirconia-silica composites calcined at 700°C are distinctly different from the composites calcined without the sodium chloride (Figure 1). This would be expected, since the impregnation with sodium chloride lowers the phase transition temperature. As a result, the crystal phase of each composite calcined at 700°C in the presence of sodium chloride is tetragonal as opposed to the amorphous composite ZS10-700 and the slightly crystalline composite ZS5-700 both calcined without the salt. The composites calcined in the presence of sodium chloride contain a reduced microporous contribution compared to the zirconia-silica composites calcined without sodium chloride. This is evidenced by comparing the cumulative frequency plots in Figure 4 and Figure 2. Thus, only 20% of the pores were smaller than 4 nm in diameter for composite ZS5-700NaCl compared to 50% when calcined without the salt. An even greater reduction in microporosity was apparent for the ZS10-700NaCl stationary phase with only 5% of the pores being less than 4 nm in diameter. As a result of the increased pore size, the surface area of the zirconia-silica composites calcined at 700°C in the presence of salt was lower than the corresponding surfaces calcined at the same temperature without the salt.

A second feature of the size exclusion curves depicted in Figure 3 is that composites ZS10 and ZS5 have distinctly different exclusion behaviour. This should be compared with the size exclusion behaviour of each composite calcined without sodium chloride (Figure 1), where each composite behaved in a similar manner. The size exclusion curve of the composite material ZS10-700NaCl (Figure 3) shows that this material had a porous structure that had an indistinct exclusion limit. This may indicate the surface contains a significant and broad macroporous region. This is shown numerically by the mean pore diameter and the standard deviation calculated from the probability plots (Table 3). A definite inclusion region was, however, apparent for this surface. By comparison, the size exclusion curve for the composite ZS5-700NaCl had a more distinct exclusion limit with an inclusion region similar to the ZS10-700NaCl composite. However, the cumulative frequency plots in Figure 4 indicate that a greater distribution of smaller pores was apparent on the surface of the ZS5 material. Thus, lowering the concentration of silicon doping decreased the mean pore diameter as apparent in a size exclusion system. The specific surface area of the composite ZS5-700NaCl was six times greater than the specific surface area of the composite ZS10-700NaCl. In addition, the pore volume of ZS5-700NaCl was twice that of the ZS10-700NaCl composite. This data is presented in Table 3. Clearly, the addition of silicon and the concentration of the silicon in the zirconia matrix has a dramatic effect on the pore structure.

Table 4

The Effect of Calcination Temperature on the Pore Structure of Zirconia-Silica Composites

Stationary Phase	Calcination Temperature (°C)	P_m (nm)	$\log(\sigma)$	S_a ($m^2 g^{-1}$)	V_p ($mL g^{-1}$)	Crystal Phase
ZS10-600NaCl	600	13.5	1.0	20.8	0.0702	Zr_{at}
ZS10-700NaCl	700	39.8	0.62	5.9	0.0589	Zr_t
ZS10-810NaCl	810	27.0	0.48	17.5	0.1179	Zr_t

A third significant feature of the exclusion curves illustrated in Figure 3 is that both the composites have different exclusion behaviour to that of pure zirconia. This is not surprising, since the addition of silicon to the zirconia matrix causes a stabilization of the amorphous phase which, in turn, leads to a surface that should maintain the microporous character to higher temperatures. Hence, the composite ZS5-700NaCl has a smaller mean pore diameter than the zirconia Zr700NaCl (Table 3). What is surprising, however, is that since the phase crystallization temperature increases monotonically with silicon doping⁴, the mean pore diameter of the composite ZS10-700NaCl is as large as it is. It would be expected that this material, calcined at 700°C, would yield a surface containing a significant distribution of smaller mesopores/micropores and a possible explanation for such deviation may depend on the decrease in the crystallization temperature resulting from the inclusion of salts. The effect of silicon concentration and salt impregnation during calcination, with respect to the crystallization temperature, has not been investigated in detail and it seems that this is warranted and will be the subject of further investigation. Further discussion regarding the macroporous nature of these supports will be considered in Part II which follows. An important difference between the pore structure of the zirconia and zirconia-silica composites that must be emphasized is that the zirconia surface has a much narrower pore size distribution.

The effect of calcination temperature on the pore structure of the zirconia-silica composites was studied using the composite ZS10. Samples were calcined in the presence of sodium chloride at 600°C, 700°C, and 810°C. Pore diameters, standard deviations, specific pore volumes and surface areas were

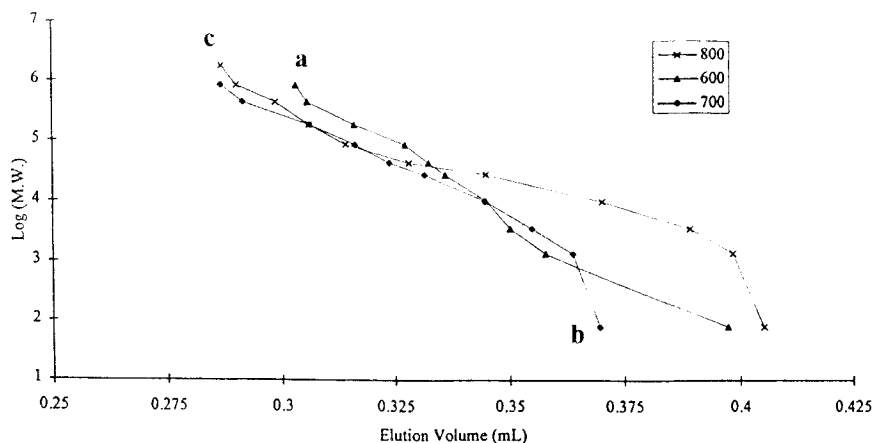


Figure 5. Size exclusion behaviour of polystyrenes illustrating the effect of calcination temperature 600°C (a), 700°C (b), 810°C (c) on the size exclusion curve for composite ZS10 calcined in a 1:1 composite:NaCl mixture. Conditions as in Figure 1.

determined as previously described and are presented in Table 4. Figure 5 shows the size exclusion curves for polystyrenes eluting from columns prepared with each of the stationary phase materials listed in Table 4. Figure 6 illustrates the cumulative pore frequency plots obtained from the size exclusion data for each material. The cumulative pore frequency plots show that a significant microporous contribution is apparent for the ZS10-600NaCl material with 50% of the pores less than 11 nm and 25% smaller than 3 nm. The mean pore diameter of this stationary phase was 13.5 nm with a very wide distribution. As the temperature of calcination increased to 700°C, the pore diameter increased and the distribution became narrower. Consequently, the surface area and the specific pore volume decreased. The mean pore diameter was 39.8 nm and the microporous region had essentially been eliminated. However, at 810°C, a decrease in the pore diameter was found rather than an increase as would be expected from previous work on zirconia¹³; in addition, the size distribution of pores narrowed.

The pore volume of ZS10-810NaCl was twice that of the material calcined at 700°C and the surface area was almost three times higher. The cumulative frequency plots in Figure 6 show that few micropores were present on the ZS10-810NaCl surface with less than 5% of the pores having diameters smaller than 3 nm. By comparison, pure zirconia that had been thermally treated in the

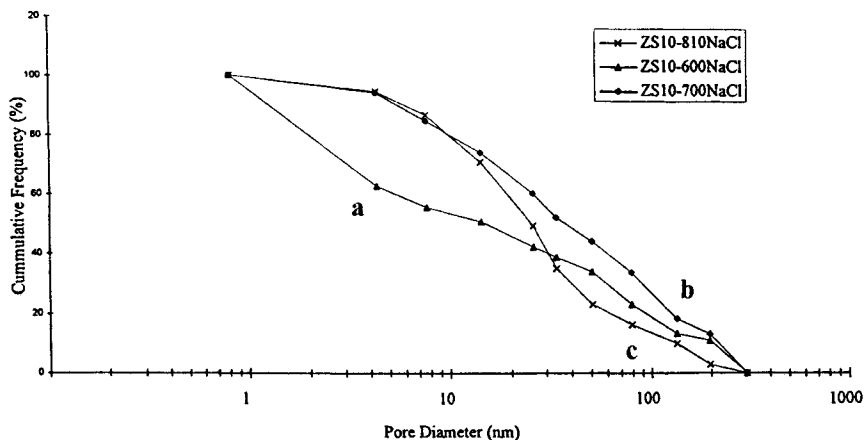


Figure 6. Cumulative pore frequency plots derived from the size exclusion data presented in Figure 5. Stationary phase ZS10-600NaCl (a), ZS10-700NaCl (b), ZS10-810NaCl (c).

Table 5

Effect of Calcination Time on the Pore Structure of Composite ZS5-700NaCl

Stationary Phase	Calcination Temperature (°C)	p_m (nm)	$\log(\sigma)$	S_a ($m^2 g^{-1}$)	V_p ($mL g^{-1}$)	Crystal Phase
1 hour ZS5-700NaCl	700	13.3	0.72	35.4	0.1178	Zr_t
5 hour ZS5-700NaCl	700	13.8	0.68	30.3	0.1047	Zr_t

Calcination of the composite ZS5-700NaCl for longer periods of time resulted in no significant change in the pore diameter and a slight decrease in the surface area and pore volume, as would be expected from previous studies¹³. In addition, the size distribution of the pores decreased slightly with the longer calcination process. These results are shown in Table 5.

To evaluate the effect of pore structure on the chromatographic performance, with respect to mass transfer into and out of the pores, column efficiencies were recorded using benzene eluting in the size exclusion system¹³

for columns prepared from the ZS10 material. As benzene is essentially unretained in 100% dichloromethane, the need to activate each surface identically with respect to the Lewis acid sites, Bronsted acid sites, and Bronsted base sites is not necessary as multimechanistic elution behaviour is minimized. Hence, peak shape is not a function of any mobile phase modifier. As a result, the elution of benzene reflects two contributions to peak broadening resulting from the column stationary phase.

The first of these is related to the passage of solute along multiple paths. This is primarily an effect due to the packing bed quality and the particle size of the support but, as each of the columns examined have been derived from the same batch of zirconia, this effect would be considered constant. Variation in column packing beds may be a factor in the results; however, all care was taken to pack the columns under identical conditions throughout.

The second contribution to peak broadening is a result of the mass transfer of the solute into and out of the pores. As each support differs widely in its pore structure, this effect should be the dominant contribution to any differences in peak broadening observed between each stationary phase support.

The variation in the height equivalent to a theoretical plate for columns prepared with composite ZS10, calcined under various conditions in both the absence and the presence of sodium chloride, are presented in Table 6. The column efficiency increased as the temperature of calcination increased for the materials calcined with the sodium chloride, whereas the opposite was observed for surfaces calcined without the sodium chloride.

This suggests that, even though increasing the calcination temperature resulted in a loss of surface area and an increase in the pore diameter when sodium chloride is included in the matrix, the efficiency improves as a direct result of an improved pore structure. By comparison, the column efficiency of a pure zirconia support was maximized at 700°C with a 1:1 mix of zirconia:sodium chloride.

The differences in column efficiencies, obtained by calcining in the presence of sodium chloride compared to the absence of sodium chloride, is quite dramatic. The salt impregnated composite calcined at 810°C had a theoretical plate height almost half that of the same composite calcined without the salt. Such a result would be related to the higher surface area and a maintenance of a mesoporous surface associated with the calcination in the presence of sodium chloride. However, no difference in efficiency was

Table 6
Column Efficiencies for Composite ZS10

Stationary Phase	Calcination Temperature (°C)	H (m)
ZS10-700	700	5.73×10^{-5}
ZS10-810	810	8.02×10^{-5}
ZS10-600NaCl	600	6.80×10^{-5}
ZS10-700NaCl	700	5.73×10^{-5}
ZS10-810NaCl	810	4.67×10^{-5}

observed for the composites calcined at 700°C with or without the sodium chloride, despite the fact that the ZS10-700NaCl material had a much lower surface area and larger pore diameter than that of the ZS10-700 material (see Tables 2 and 4).

CONCLUSION

The pore structure of zirconia-silica composites, prepared using the procedure described, is extremely complicated. Pore dimensions vary as a function of the silicon doping and the thermal treatment. Hence, to prepare stationary phase supports suitable for chromatography, knowledge of the pore structure is vital in obtaining efficient separations.

Comparisons in separation selectivities between solutes as a function of silicon loading may only be made after similar surfaces have been prepared.

We have shown that the pore structure of these composites is extremely temperature sensitive after crystallization, but the inclusion of sodium chloride during the calcination process stabilizes the surface to a greater extent. A knowledge of the crystal phase, silicon doping, and, ultimately, to the pore structure is extremely important before using these materials for chromatographic purposes.

ACKNOWLEDGMENTS

The authors express their gratitude for support from the Center for Instrumental and Developmental Chemistry, School of Physical Sciences, Queensland University of Technology (QUT). We also wish to acknowledge the support of a QUT Meritorious Research Award. One of the authors (RAS) would like to gratefully acknowledge the receipt of a QUT Postdoctoral Research Fellowship. We would like to thank Mr. Shane Russell for his assistance in the thermal gravimetric analysis.

REFERENCES

1. J. Nawrocki, M. P. Rigney, A. McCormick, P. W. Carr, *J. Chromatogr.*, **657**, 229 (1993).
2. S. Kaneko, T. Mitsuzawa, S. Ohmori, M. Nakamura, K. Nobuhara, M. Masatani, *J. Chromatogr.*, **669**, 1 (1994).
3. R. A. Shalliker, L. Rintoul, G. K. Douglas, S. C. Russell, *J. Mater. Sci.*, **32(1)**, 2949 (1997).
4. R. A. Shalliker, G. K. Douglas, L. Rintoul, S. C. Russell, (submitted for publication).
5. R. A. Shalliker, G. K. Douglas, L. Rintoul, P. R. Comino, P. E. Kavanagh, *J. Liq. Chromatogr.*, **20(10)**, 1471 (1997).
6. I. Halász, K. Martin, *Agnew. Chem. Int. Ed. Eng.*, **17**, 901 (1978).
7. J. Nawrocki, M. P. Rigney, A. McCormick, P. W. Carr, *J. Chromatogr.*, **657**, 229 (1993).
8. P. D. L. Mercera, J. G. Van Ommen, E. B. M. Doesburg, A. J. Burggraaf, J. R. H. Ross, *Appl. Catal.*, **57**, 127 (1990).
9. J. Livage, K. Doc, C. Mazieres, *J. Amer. Ceram. Soc.*, **51**, 349 (1968).
10. P. Kunda, D. Pal, S. Sen, *J. Mater. Sci.*, **23**, 1539 (1988).
11. H. C. Wang, K. L. Lin, *J. Mater. Sci.*, **26**, 2501 (1991).

12. S. W. Lee, R. A. Condrate, Sr., *J. Mater. Sci.*, **23**, 2951 (1988).
13. R. A. Shalliker, G. K. Douglas, *J. Liq. Chromatogr.*, **20(11)**, 1651 (1997).
14. R. A. Shalliker, G. K. Douglas, P. R. Comino, P. E. Kavanagh, *Powder Technology*, **91(1)**, 17 (1997).

Received July 7, 1997

Accepted October 16, 1997

Manuscript 4537